Pharmaceutical Sciences and Drug Design
ISSN: 3062-4428
2025, Volume 5, Page No: 269-282

Available online at: www.galaxypub.co/page/journals

Galaxy Publication

Galaxy Publication

Discovery of Novel Serine Acetyltransferase Inhibitors through Virtual Screening and Structure–Activity Analysis

Pedro Almeida[1], Joana Figueiredo[2]*, Miguel Costa[1]

[1]Department of Drug Development, Faculty of Health Sciences, University of Coimbra, Coimbra, Portugal.
[2]Department of Pharmaceutical Sciences, Faculty of Pharmacy, University of Lisbon, Lisbon, Portugal.

***E-mail** ✉ joana.figueiredo@outlook.com

Received: 14 October 2024; **Revised:** 19 January 2025; **Accepted:** 22 January 2025

ABSTRACT

Numerous bacteria and actinomycetes rely on L-cysteine biosynthesis to enhance their tolerance to antibacterial agents and to sustain persistent infections, a phenomenon that contributes to the emergence of antimicrobial resistance—one of the most critical global public health challenges. As the enzymatic pathway responsible for L-cysteine production is absent in mammalian cells, it represents an attractive and selective target for therapeutic intervention. In this study, we describe the identification of a series of inhibitors targeting serine acetyltransferase (SAT) from Salmonella typhimurium, the enzyme responsible for catalyzing the rate-limiting step in L-cysteine biosynthesis. These inhibitors were discovered through a virtual screening campaign conducted on an in-house chemical library, which yielded seven structurally diverse hit compounds. Subsequent evaluation of analogues structurally related to hit compound 5—either sourced from the original library or generated through medicinal chemistry optimization—enabled the establishment of preliminary structure–activity relationships and led to a marked enhancement of inhibitory potency relative to the initial hit. Despite these improvements at the enzymatic level, the most advanced compound did not exhibit detectable antibacterial activity in a Gram-negative model organism, highlighting the need for further optimization and investigation.

Keywords: Antimicrobial resistance, Adjuvant therapies, Non-essential targets, Cysteine biosynthesis, Serine acetyltransferase

How to Cite This Article: Almeida P, Figueiredo J, Costa M. Discovery of Novel Serine Acetyltransferase Inhibitors through Virtual Screening and Structure–Activity Analysis. Pharm Sci Drug Des. 2025;5:269-82. https://doi.org/10.51847/qKRpSdRxhm

Introduction

Cysteine is an essential amino acid that mammals are unable to synthesize de novo and therefore must obtain from dietary sources. It serves as a fundamental component of numerous biomolecules and cofactors, including S-adenosylmethionine, coenzyme A, biotin, lipoic acid, and thiamine pyrophosphate, and constitutes the reactive moiety of key detoxifying molecules such as glutathione and mycothiol. Beyond its universal biological importance, cysteine plays a particularly critical role in the survival of certain facultative intracellular pathogens, which must cope with nutrient deprivation and oxidative stress within macrophages. Under such hostile conditions, disruption of bacterial adaptive mechanisms can impair infectivity and increase susceptibility to antibacterial agents. Although enzymes involved in cysteine biosynthesis are dispensable during in vitro growth or acute infection, they become essential during bacterial persistence within the host [1, 2].

Over the past several years, substantial evidence has demonstrated that attenuation or inhibition of cysteine biosynthesis adversely affects bacterial fitness and virulence [2-8]. For example, deletion mutants of cysteine biosynthetic enzymes exhibit reduced virulence, as observed for cysH in Mycobacterium tuberculosis [9] and cysI or cysK in Brucella melitensis [10], or increased sensitivity to oxidative stress, as reported for the cysI mutant of B. melitensis [10]. Notably, cysteine biosynthesis has also been implicated in the development of antibiotic

resistance. In Salmonella typhimurium, genetic disruption of this pathway resulted in a compromised oxidative stress response, leading to diminished antibiotic resistance in both vegetative and swarm cell populations [11]. Collectively, these observations suggest that targeting cysteine biosynthesis may offer a dual therapeutic benefit by enhancing the efficacy of existing antibacterial agents and limiting the emergence of antimicrobial resistance. Given that antimicrobial resistance (AMR) is widely regarded as a major impending global health crisis, the therapeutic relevance of inhibiting cysteine biosynthesis is further underscored. Current projections estimate that AMR could result in up to 10 million deaths annually by 2050 if novel intervention strategies are not implemented [12-14]. In addition to identifying new druggable targets through conventional drug discovery efforts, an effective strategy to combat AMR involves the development of unconventional approaches, such as adjuvant therapies. These agents typically exhibit weak or no intrinsic antibacterial activity but act on non-essential targets associated with bacterial virulence and persistence following host colonization [15-18]. Such targets are not required for bacterial survival under normal conditions but become critical during infection, where they help mitigate the deleterious effects of antibiotics [18]. The use of adjuvants offers several advantages, including suppression of intrinsic resistance and expansion of the antibacterial spectrum of existing drugs [19]. Furthermore, adjuvants may enable dose reduction of antibiotics with known toxicity, thereby minimizing adverse effects [20]. Since non-essential targets are not directly linked to bacterial viability, they are also less prone to selective pressure and resistance development [21].

In the terminal stages of cysteine biosynthesis, serine acetyltransferase (SAT) catalyzes the transfer of an acetyl group from acetyl-CoA to L-serine, generating O-acetylserine (OAS). Subsequently, O-acetylserine sulfhydrylase (OASS) mediates the β-substitution of OAS with sulfide to produce cysteine and acetate. Significant efforts by our research group [22-25] and others [26-29] have focused on the identification of potent and selective OASS inhibitors for use as antibacterial agents—particularly against M. tuberculosis—or as adjuvants. These studies culminated in the discovery of UPAR-415, the most potent inhibitor of S. typhimurium OASS reported to date **(Figure 1)** [30]. Despite its strong biochemical activity, UPAR-415 failed to demonstrate comparable efficacy in bacterial cell assays. Nevertheless, recent evidence suggests that UPAR-415 may function as a colistin adjuvant in pathogen infections (manuscript submitted). Preliminary investigations indicated that limited cellular permeability likely hindered the compound's ability to reach intracellular targets, a common challenge in antibacterial drug discovery. In light of these findings, attention was redirected toward the upstream step of cysteine biosynthesis catalyzed by SAT. To date, SAT inhibition has been relatively underexplored, and the available inhibitors exhibit only modest activity [26, 31-33]. SAT facilitates the acetylation of the hydroxyl group of L-serine using acetyl-CoA, yielding OAS, the activated form of serine. In contrast to OASS inhibition, targeting SAT is expected not only to reduce cysteine production downstream but also to prevent the accumulation of OAS, which is converted to N-acetylserine (NAS) and acts as an inducer of the cysteine biosynthetic operon [34]. Structurally, SAT assembles as a dimer of trimers, comprising an N-terminal α-helical domain and a C-terminal left-handed α-helix domain that terminates in a flexible, disordered tail. This C-terminal region interacts with OASS-A at its active site, resulting in competitive inhibition [35, 36]. Our initial strategy to identify SAT inhibitors involved the virtual screening of a focused commercial compound library [37], inspired by earlier studies that reported promising outcomes using similar methodologies [27, 33]. In this first campaign, three ChemDiv-focused libraries encompassing 91,243 compounds were screened, leading to the identification of six molecules with IC_{50} values below 100 μM, as determined by an indirect Ellman's reagent-based assay [37]. Notably, one of these compounds also exhibited measurable growth inhibition against Escherichia coli. Building on this experience, we applied a comparable virtual screening approach to an in-house chemical library originally designed to target proteins other than SAT. In recent years, repurposing drug and chemical libraries has emerged as a highly effective strategy in drug discovery, allowing both academic institutions and pharmaceutical companies to reassess existing compounds for alternative biological applications. This approach offers the significant advantage of revitalizing molecules that may otherwise remain unexplored, often with prior chemical and biological characterization already available. Although smaller in size than commercial libraries, the virtual screening of our in-house collection successfully identified a limited number of promising hit compounds **(Figure 2)**. Subsequent structure–activity relationship analyses were conducted using both existing analogues from the library and newly synthesized derivatives.

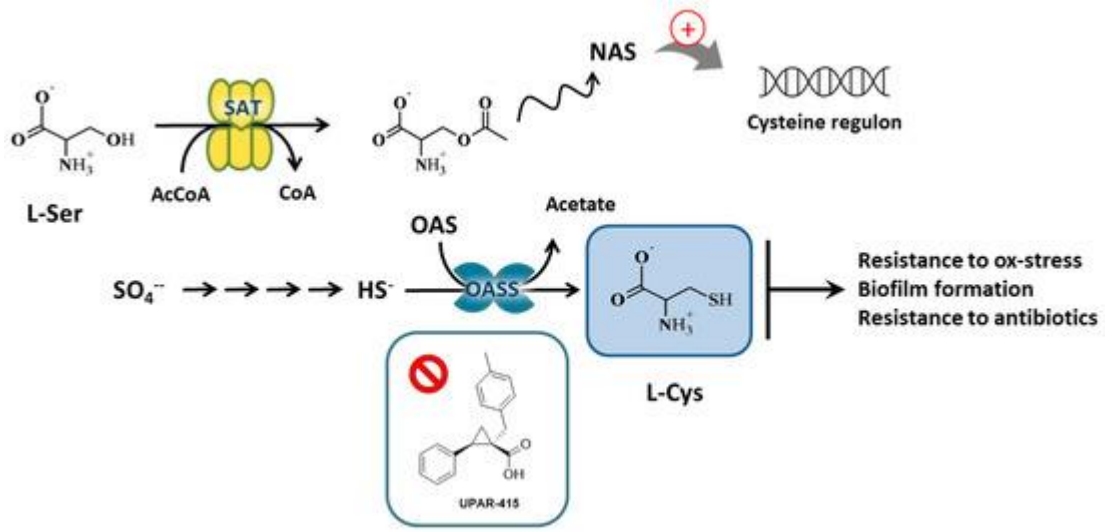

Figure 1. Representation of the reductive sulfate assimilation pathway operating in *Salmonella*. Sulfate ions are actively transported into the cell and sequentially reduced to bisulfide through a series of enzymatic reactions.

Serine acetyltransferase (SAT) catalyzes the acetylation of L-serine, yielding O-acetylserine (OAS), which spontaneously equilibrates with N-acetylserine (NAS), the transcriptional inducer of the cysteine regulon. The subsequent β-replacement reaction between OAS and HS^-, mediated by O-acetylserine sulfhydrylase (OASS), produces L-cysteine. Cysteine and its biosynthetic network are involved in several infection-related processes, including oxidative stress defense, biofilm development, and resistance to antibacterial agents. UPAR-415 functions as a competitive inhibitor of OASS.

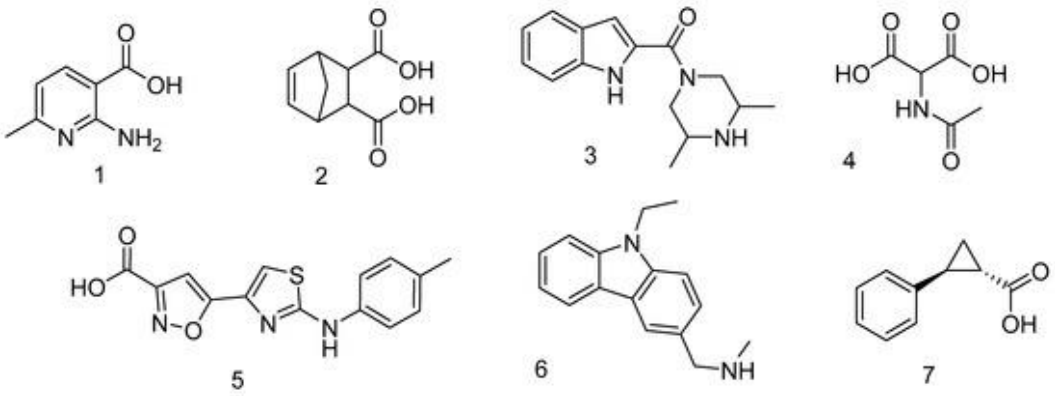

Figure 2. Chemical structures of hit compounds identified through virtual screening.

Materials and Methods

Enzyme preparation and activity assay

Serine acetyltransferase (SAT) from Salmonella enterica serovar Typhimurium was expressed as a trxA fusion protein as previously reported [37] and was >95% pure by SDS-PAGE. Enzyme activity was monitored using a spectrophotometric indirect assay that detects the absorbance at 412 nm produced by the reduction of 5,5'-dithiobis(2-nitrobenzoic acid) (Ellman's reagent) by the product coenzyme A [37]. All assays contained 5% DMSO, which did not affect enzyme activity (data not shown). Substrate concentrations were set to their Km values to enhance assay sensitivity for both competitive and uncompetitive inhibition modes [38]. The dependence of relative reaction rate on inhibitor concentration was fitted to Equation (1) to determine IC_{50} values.

$$\frac{vi}{v0} = \frac{1}{1 + \frac{[I]}{IC50}} \quad (1)$$

The inhibition mode was established by fitting initial reaction rates versus acetyl CoA concentration (at fixed 1 mM L-serine) in the presence of varying inhibitor levels (1/3 IC50 ≥ [inhibitor] ≤ 3 IC50) to equations describing competitive, uncompetitive, or non-competitive inhibition [38]. The competitive inhibition equation (Equation (2)) was applied to calculate the Ki value for compound 5.

$$v_0 = \frac{Vmax \cdot [acetyl - CoA]}{[acetyl - CoA] + (Km \cdot \alpha)} \quad (2)$$

where $\alpha = 1 + (\frac{[comp5]}{k_i})$.

Chemistry

All reagents were obtained from Sigma-Aldrich, Alfa-Aesar, and Enamine in reagent grade and used without further purification unless specified. Anhydrous solvents were prepared by distillation over suitable drying agents. Microwave-assisted reactions were conducted in a CEM Discover microwave synthesizer. Reaction progress was followed by thin-layer chromatography on silica gel-coated aluminum plates (SUPELCO Analytical, Sigma-Aldrich) under UV light at 254 and 365 nm. Purification of intermediates and final compounds, when required, was performed by flash column chromatography on silica gel (0.040–0.063 mm) using suitable eluent mixtures. 1H NMR and 13C NMR spectra were acquired on a BRUKER AVANCE instrument at 300 or 400 MHz (1H) and 100 MHz (13C), with TMS as internal standard. Multiplicities are reported as: s = singlet, d = doublet, dd = doublet of doublets, t = triplet, q = quartet, m = multiplet, br = broad. HPLC/MS analyses employed an Agilent 1100 series system (Waters Symmetry C18 column, 3.5 µm, 4.6 × 75 mm) coupled to an Applied Biosystem/MDS SCIEX API 150EX mass spectrometer. High-resolution mass spectrometry was performed on a Thermo LTQ Orbitrap XL. All tested compounds were ≥95% pure by HPLC/MS.

Analytical data for compounds 8–20 and 23–27 have been reported previously [39-41].

- Ethyl 5-acetylisoxazole-3-carboxylate (25): A solution of triethylamine (4 mL, 29 mmol) in THF (10 mL) was added dropwise to a mixture of butynone 23 (2.3 mL, 29 mmol) and ethyl-2-chloro-2-(hydroxyimino)acetate 24 (4.39 g, 29 mmol) in THF (37.5 mL). The mixture was stirred at room temperature for 3 h, then concentrated. The residue was extracted with ethyl acetate (3 × 50 mL), and the combined organics were dried over anhydrous Na2SO4, filtered, and evaporated. Purification by flash chromatography (ethyl acetate/petroleum ether 7:93) gave the product as a white powder in 50% yield. 1H NMR (400 MHz, CDCl3) δ 7.26 (s, J = 2.0 Hz, 1H), 4.47 (q, J = 7.1 Hz, 2H), 2.65 (s, 3H), 1.43 (t, J = 7.1 Hz, 3H).
- Ethyl 5-(2-bromoacetyl)isoxazole-3-carboxylate (26): To a solution of 25 (2.65 g, 14.47 mmol) in acetonitrile (26.8 mL) cooled in an ice bath, p-toluenesulfonic acid monohydrate (2.49 g, 14.47 mmol) and N-bromosuccinimide (2.58 g, 14.47 mmol) were added portionwise. The mixture was refluxed for 5 h, then concentrated and purified by flash chromatography (gradient of ethyl acetate in petroleum ether) to afford the product as a yellow powder in 58% yield. 1H NMR (300 MHz, DMSO-d6) δ 7.89 (s, 1H), 4.87 (s, 2H), 4.41 (dt, J = 12.4, 4.5 Hz, 2H), 1.34 (t, J = 7.1 Hz, 3H).
- Ethyl 5-(2-aminooxazol-4-yl)isoxazole-3-carboxylate (27): A mixture of 26 (315 mg, 1.2 mmol) and urea (721 mg, 12 mmol) in anhydrous DMF (3.14 mL) was refluxed for 2 h and cooled to room temperature. Aqueous 5% LiCl (32 mL) was added, followed by extraction with ethyl acetate (4 × 10 mL). The organics were washed with water and brine, dried over Na2SO4, filtered, and concentrated. Flash chromatography yielded the product as a yellow powder in 77% yield. 1H NMR (300 MHz, DMSO-d6) δ 8.15 (s, 1H), 7.07 (s, 2H), 6.89 (s, 1H), 4.37 (dd, J = 13.8, 6.8 Hz, 2H), 1.32 (t, J = 6.9 Hz, 3H).
- General procedure for Buchwald–Hartwig amination (compounds 21a–e): In a microwave vial, the appropriate 2-aminooxazole (1 equiv), aryl halide (0.5 equiv), and base (1 equiv) in anhydrous toluene (2.5 mL/mmol) and t-butanol (0.5 mL/mmol) were stirred under argon for 15 min. The catalyst (0.1 equiv) was added, and the mixture was microwaved (130 °C, 15 min, 250 psi, 300 W). After TLC indicated completion, water was added, and the mixture was extracted with ethyl acetate (3 × 10 mL). The organics were washed with water and brine, dried over Na2SO4, filtered, concentrated, and purified by flash chromatography.
- Ethyl 5-(2-(phenylamino) oxazol-4-yl)isoxazole-3-carboxylate (21a): Flash chromatography (ethyl acetate/petroleum ether 1:9) gave a yellow solid in 24% yield. 1H NMR (400 MHz, Acetone-d6) δ 9.41 (s, 1H),

8.17 (s, 1H), 7.76 (d, J = 7.9 Hz, 2H), 7.36 (t, J = 7.9 Hz, 2H), 7.12–6.75 (m, 2H), 4.43 (q, J = 7.1 Hz, 2H), 1.39 (t, J = 7.1 Hz, 3H). 13C NMR (100.6 MHz, Acetone-d6) δ 20.8, 62.4, 101.5, 117.4, 122.4, 129.8, 132.7, 136.9, 156.5, 156.6, 158.1, 159.3, 165.1. HRMS (ESI) calcd for C15H13N3O4 [M + H]+ 300.0906, found 300.1112.

- Ethyl 5-(2-((3,5-dichlorophenyl)amino)oxazol-4-yl)isoxazole-3-carboxylate (21b): Flash chromatography (ethyl acetate/petroleum ether 1:9) gave an orange powder in 30% yield. 1H NMR (300 MHz, CDCl3) δ 7.82 (s, 1H), 7.51 (d, J = 1.6 Hz, 2H), 7.07 (s, 1H), 7.02 (s, 2H), 4.48 (q, J = 7.1 Hz, 2H), 1.45 (t, J = 7.1 Hz, 3H). 13C NMR (100.6 MHz, CDCl3) δ 18.5, 62.1, 101.3, 108.8, 119.8, 120.2, 128.0, 139.9, 150.1, 154.8, 156.8, 158.2, 160.5. HRMS (ESI) calcd for C15H11Cl2N3O4 [M + H]+ 368.0126, found 368.0520.
- Ethyl 5-(2-((4-fluorophenyl) amino) oxazol-4-yl) isoxazole-3-carboxylate (21c): Flash chromatography (ethyl acetate/petroleum ether 1:9) gave a slightly orange powder in 8% yield. 1H NMR (300 MHz, CDCl3) δ 7.77 (s, 1H), 7.51 (dd, J = 8.4, 4.2 Hz, 2H), 7.07 (t, J = 8.5 Hz, 2H), 6.98 (s, 1H), 6.92 (s, 1H), 4.47 (q, J = 7.1 Hz, 2H), 1.44 (t, J = 7.1 Hz, 3H). 13C NMR (100.6 MHz, CDCl3) δ 18.9, 62, 100.8, 108.2, 121.0, 121.2, 127.8, 139.9, 150.1, 154.8, 157.3, 159.2, 160.8. HRMS (ESI) calcd for C15H12FN3O4 [M + H]+ 318.0811, found 318.0822.
- Ethyl 5-(2-((3,5-dimethylphenyl)amino)oxazol-4-yl)isoxazole-3-carboxylate (21d): Flash chromatography (ethyl acetate/petroleum ether 1:9) gave a yellow powder in 35% yield. 1H NMR (300 MHz, DMSO-d6) δ 10.28 (s, 1H), 8.42 (s, 1H), 7.25 (s, 2H), 7.10 (s, 1H), 6.63 (s, 1H), 4.39 (q, J = 7.1 Hz, 2H), 2.26 (s, 6H), 1.34 (t, J = 7.1 Hz, 3H). 13C NMR (100.6 MHz, DMSO-d6) δ 18.8, 21.8, 21.9, 61.8, 100.8, 112.8, 121.4, 126.2, 138.8, 140.1, 150.8, 155, 156.8, 159.2, 160.8. HRMS (ESI) calcd for C17H17N3O4 [M + H]+ 328.1219, found 328.1401.
- Ethyl 5-(2-(pyridin-4-ylamino)oxazol-4-yl)isoxazole-3-carboxylate (21e): Flash chromatography (ethyl acetate/petroleum ether 1:1 → 100%) gave a yellow powder in 15% yield. 1H NMR (400 MHz, Acetone-d6) δ 8.47 (d, J = 6.2 Hz, 2H), 8.27 (s, 1H), 7.73 (d, J = 6.3 Hz, 2H), 7.07 (s, 1H), 4.44 (q, J = 7.1 Hz, 2H), 1.40 (t, J = 7.1 Hz, 3H). 13C NMR (100.6 MHz, Acetone-d6) δ 21, 62.4, 101.3, 109.0, 125.4, 139.2, 150.1, 155.6, 156.6, 158.1, 159.3, 160.5. HRMS (ESI) calcd for C14H12N4O4 [M + H]+ 301.0858, found 301.0999.
- General procedure for ester hydrolysis (compounds 22a–e): The appropriate ester (1 equiv) and LiOH·H2O (4 equiv) were stirred in THF/MeOH/H2O (3:1:1, 1 mL/mmol) at room temperature until TLC showed complete consumption of starting material. The mixture was concentrated, diluted with water, acidified with 2 N HCl, and extracted with ethyl acetate (3 × 10 mL). Evaporation provided the carboxylic acids in sufficient purity.
- 5-(2-(phenylamino) oxazol-4-yl) isoxazole-3-carboxylic acid (22a): Yellow powder (37% yield). 1H NMR (400 MHz, DMSO-d6) δ 10.45 (s, 1H), 9.47 (s, 1H), 8.42 (s, 1H), 7.66 (d, J = 7.8 Hz, 2H), 7.34 (t, J = 7.9 Hz, 2H), 7.00 (dd, J = 15.0, 7.6 Hz, 2H). 13C NMR (101 MHz, DMSO-d6) δ 164.5, 160.6, 157.4, 138.8, 132.1, 129.0, 128.9, 121.6, 116.8, 101.2. HRMS (ESI) calcd for C13H9N3O4 [M + H]+ 272.0593, found 272.0606.
- 5-(2-((3,5-dichlorophenyl)amino)oxazol-4-yl)isoxazole-3-carboxylic acid (22b): Light yellow powder (60% yield). 1H NMR (400 MHz, DMSO-d6) δ 11.01 (s, 1H), 8.49 (s, 1H), 7.72 (d, J = 1.8 Hz, 2H), 7.19 (t, J = 1.8 Hz, 1H), 7.03 (s, 1H). 13C NMR (101 MHz, DMSO-d6) δ 160.4, 156.2, 141.0, 134.2, 132.5, 127.9, 124.0, 120.5, 114.7, 101.2. HRMS (ESI) calcd for C13H7Cl2N3O4 [M + H]+ 339.9814, found 339.9986.
- 5-(2-((4-fluorophenyl) amino)oxazol-4-yl)isoxazole-3-carboxylic acid (22c): Yellow powder (81% yield). 1H NMR (400 MHz, Acetone-d6) δ 9.48 (s, 1H), 8.18 (s, 1H), 7.85–7.77 (m, 2H), 7.19–7.11 (m, 2H), 7.01 (s, 1H). 13C NMR (101 MHz, Acetone-d6) δ 166.0, 161.0, 160.1, 158.6, 158.0, 136.3, 132.3, 129.8, 119.6, 119.5, 116.4, 116.2, 102.2. HRMS (ESI) calcd for C13H8FN3O4 [M + H]+ 290.0499, found 290.0509.
- 5-(2-((3,5-dimethylphenyl)amino)oxazol-4-yl)isoxazole-3-carboxylic acid (22d): Yellow powder (68% yield). 1H NMR (400 MHz, DMSO-d6) δ 10.28 (s, 1H), 8.41 (s, 1H), 7.26 (s, 2H), 7.04 (s, 1H), 6.64 (s, 1H), 2.27 (s, 6H). 13C NMR (101 MHz, DMSO-d6) δ 165.0, 161.0, 157.9, 157.7, 139.1, 138.4, 132.4, 128.5, 123.8, 115.0, 101.6, 21.6. HRMS (ESI) calcd for C15H13N3O4 [M + H]+ 300.0906, found 300.1002.
- 5-(2-(pyridin-4-ylamino) oxazol-4-yl)isoxazole-3-carboxylic acid (22e): Yellow powder (63% yield). 1H NMR (300 MHz, DMSO-d6) δ 12.58 (s, 1H), 8.71 (s, 1H), 8.66 (d, J = 7.2 Hz, 2H), 8.12 (d, J = 5.6 Hz, 2H), 7.20 (s, 1H). 13C NMR (101 MHz, DMSO-d6) δ 163.6, 160.5, 157.5, 155.0, 143.0, 134.2, 128.2, 112.2, 102.0. HRMS (ESI) calcd for C12H8N4O4 [M + H]+ 273.0545, found 273.0628.

Biology

Reference bacterial strains were prepared by inoculating 4–5 morphologically uniform colonies into MHB and M9 media, followed by incubation at 37 °C with shaking at 240 rpm until exponential growth was achieved.

Cultures were then harvested by centrifugation at 2000 rpm for 20 min at 4 °C. The resulting pellets were resuspended in fresh MHB or M9 medium, and cell density was determined spectrophotometrically. An optical density at 600 nm in the range of 0.08–0.13 was taken to correspond to approximately 10^8 CFU/mL [42].

The bacterial suspensions were subsequently diluted by transferring 100 µL into 9.9 mL of the appropriate medium to obtain a final concentration of 10^6 CFU/mL. Aliquots of 50 µL were dispensed into the wells of microtiter plates within 30 min of preparation, resulting in an inoculum of 5×10^5 CFU/mL per well, in accordance with CLSI recommendations [42]. The antibacterial activity of compounds 22a, 22b, and 22d was evaluated using a minimum inhibitory concentration (MIC) assay. Briefly, each well of a microtiter plate was filled with 49 µL of either M9 or MHB medium, followed by the addition of 1 µL of each compound, previously prepared in DMSO. This procedure generated a concentration range spanning from 128 µg/mL to 0.25 µg/mL, while maintaining a final bacterial density of 5×10^5 CFU/mL in a total volume of 100 µL. Appropriate growth and sterility controls were included in each experiment. For every bacterial strain tested, three independent experiments were performed, each consisting of three technical replicates.

Results and Discussion

Identification of Hit compounds through virtual screening

Because the amino acid sequence of serine acetyltransferase is highly conserved among bacterial species [43], our in-house compound collection was screened in silico using the crystal structures of SAT from *E. coli* (EcSAT, PDB: 1T3D) and *H. influenzae* (HiSAT, PDB: 1SSM). Docking protocols and parameters were consistent with those previously established by our group [37]. This computational workflow led to the selection of seven candidate molecules, which were subsequently evaluated experimentally using recombinant SAT from *S. typhimurium*. The enzyme displayed kinetic constants of $K_{m,Ser} = 1.07 \pm 0.15$ mM, $K_{m,AcCoA} = 0.17 \pm 0.04$ mM, and $k_{cat} = 3813 \pm 169$ min^{-1} [37]. To ensure detection of inhibitors acting through different mechanisms, both substrates were used at concentrations corresponding to their respective Km values during the initial screening.

A common structural feature emerged among the identified candidates, as six of the seven compounds possessed a carboxylate group, indicating a likely role for this functionality in productive enzyme binding. To prioritize compounds for further investigation, enzymatic inhibition by compounds 1–7 was measured at a single concentration of 1 mM **(Table 1).** Two molecules, compounds 5 and 7, reduced SAT activity by more than 40% and were therefore selected for detailed potency assessment. Subsequent IC_{50} measurements confirmed compound 5 as the most effective inhibitor, with an IC_{50} of 110 ± 0 µM, whereas compound 7 showed weak inhibition, with an IC_{50} greater than 2 mM.

Kinetic analysis demonstrated that compound 5 inhibits SAT competitively with respect to acetyl-CoA, yielding a Ki value of 64 ± 12 µM **(Figure 3).** Molecular modeling studies supported this mechanism, indicating that the compound is capable of interacting with both the L-serine and acetyl-CoA binding regions of the enzyme. The bent, L-shaped scaffold of compound 5 allows partial occupation of the acetyl-CoA pocket, while its carboxylate moiety reproduces key interactions made by the carboxyl group of L-serine **(Figure 4).** This binding configuration is consistent with competition for acetyl-CoA binding, although additional contacts within the pocket may also contribute to inhibition.

Compound 5 originates from a family of 2-aminothiazole derivatives previously developed in the context of antitubercular drug discovery and synthesized for structure–activity relationship studies [39]. Notably, despite the strong antimycobacterial activity displayed by other members of this series, compound 5 itself lacks activity against *M. tuberculosis*. This absence of antibacterial activity is advantageous for repurposing purposes, as it minimizes the risk of unintended off-target effects.

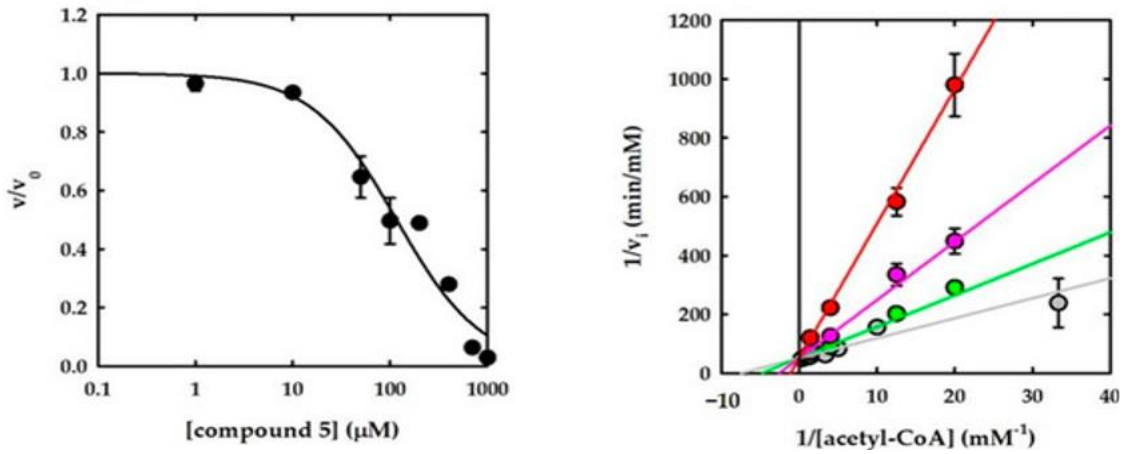

a) b)

Figure 3. Inhibition profile of compound 5. (a) Relative initial reaction velocity as a function of compound 5 concentration. Experimental data were fitted to Equation 1, yielding an IC_{50} value of 110 ± 0 μM. (b) Initial reaction rates measured at increasing acetyl-CoA concentrations in the absence of inhibitor (grey symbols) and in the presence of compound 5 at 30 μM (green symbols), 100 μM (pink symbols), and 300 μM (red symbols). Data were fitted using the linearized form of Equation 2, providing a Ki value of 64 ± 12 μM.

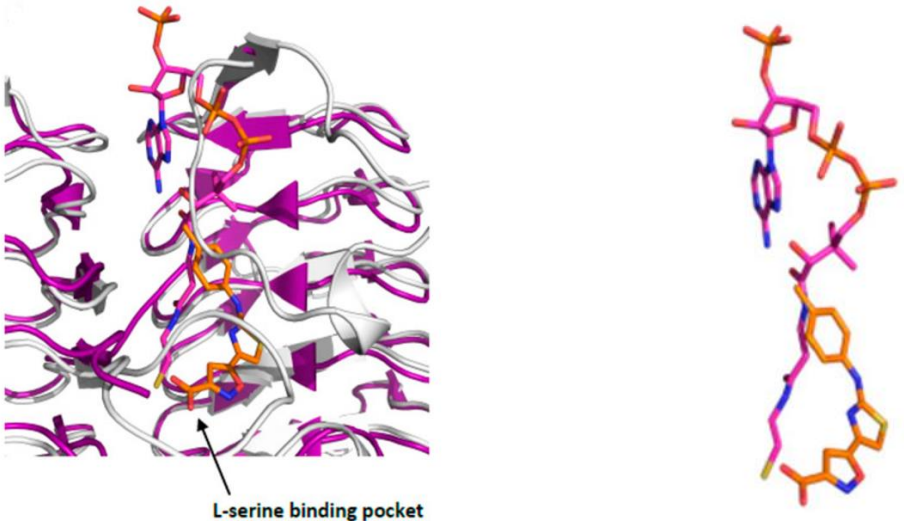

a) b)

Figure 4. (a) Predicted binding orientation of compound 5 within the acetyl-CoA binding site of EcSAT, obtained by structural alignment of the enzymes corresponding to PDB codes 1T3D and 1SSM. (b) Superposition of the docked pose of compound 5 with the crystallographic structure of acetyl-CoA.

Table 1. Inhibitory effects of virtual screening–derived compounds on SAT activity.

Compound	Percentage Inhibition at 1 mM	IC_{50} (μM)	K_i (μM)	Inhibition Mechanism
1	19.4 ± 1	ND	ND	-
2	34.9 ± 6	ND	ND	-
3	31.4 ± 5	ND	ND	-
4	18.7 ± 6	ND	ND	-
5	98.6 ± 0	110 ± 0	64 ± 12	Competitive with acetyl-CoA
6	23.6 ± 0	ND	ND	-
7	42 ± 5	>2 mM	ND	-

[a] ND = Not Determined.

Expansion of the initial hit

The optimization strategy aimed at identifying an improved inhibitor of StSAT was pursued through a two-stage approach. Initially, a selection of compound 5 analogues already present in the in-house collection was evaluated to establish preliminary structure–activity relationships (SAR). Subsequently, insights derived from this analysis guided the targeted synthesis of additional derivatives. Thirteen structurally related compounds were selected from the internal library and examined for their inhibitory activity against StSAT **(Table 2).** Within this subset, the carboxyl group was conserved either in its free acid form or converted into ester or amide functionalities. In selected derivatives, the isoxazole moiety was replaced with an N-methylpyrazole to probe the influence of heterocycle variation. Moreover, the impact of introducing small electron-withdrawing substituents on the phenyl ring linked to the 2-aminothiazole core was systematically investigated.

Most of the tested analogues exhibited enhanced inhibitory potency relative to the parent compound 5. Notably, compounds 18 and 19—featuring substitution of the 2-aminothiazole ring with a 2-aminooxazole scaffold—emerged as the most effective inhibitors within this series. Encouraged by these results, further synthetic efforts focused on expanding this chemical class. Specifically, additional analogues derived from the 2-aminooxazole cores of compounds 18 and 19 were designed and prepared using a previously reported synthetic methodology [40], which is particularly well suited for the functionalization of substituted 2-aminooxazoles **(Scheme 1).**

This second set of compounds comprised 3-carboxylisoxazole derivatives bearing a range of aromatic and heteroaromatic substituents linked to the nitrogen atom of the 2-aminooxazole moiety (21a–e, 22a–e). For this initial substitution study, pyridine and phenyl groups—either unsubstituted or functionalized with electron-donating or electron-withdrawing substituents—were selected to assess their influence on enzyme inhibition.

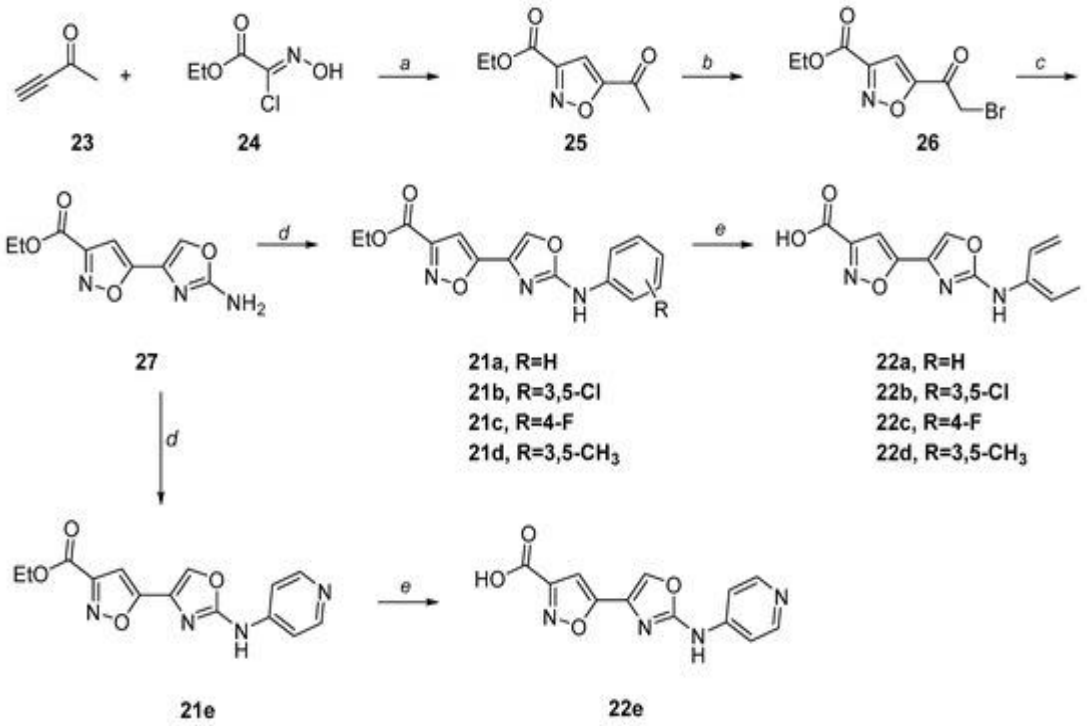

Scheme 1. a Reagents and conditions: (a) triethylamine, tetrahydrofuran, room temperature; (b) N-bromosuccinimide, *p*-toluenesulfonic acid, acetonitrile, reflux; (c) urea, dimethylformamide, microwave irradiation (120 °C, 300 W), 3 min, 49% yield; (d) appropriate bromobenzene derivative or 4-bromopyridine (21e), sodium *tert*-butoxide, X-Phos Pd G2, *tert*-butanol/toluene, microwave irradiation (130 °C, 300 W), 15 min, 8–35% yield; (e) LiOH, THF/H_2O/MeOH (3:1:1), room temperature, 3 h, quantitative yield.

Table 2. Inhibitory activity of compound 5 analogues against StSAT.

Cpd	Structure	IC_{50} (μM)	Cpd	Structure	IC_{50} (μM)

8	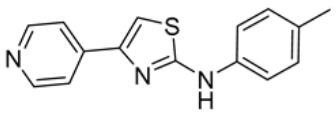	>400	**15**	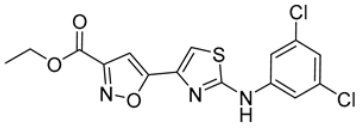	18 ± 2
9	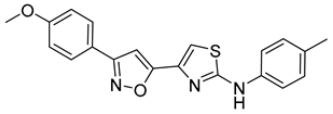	12 ± 2	**16**	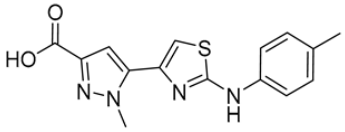	184 ± 13
10	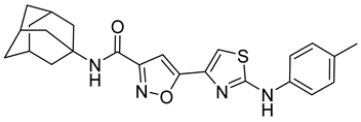	9 ± 3	**17**	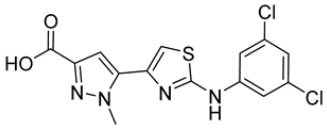	21 ± 5
11	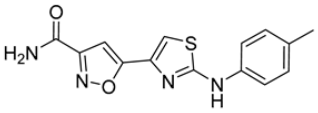	26 ± 4	**18**	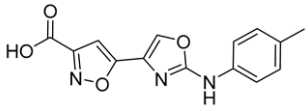	1.0 ± 0.2
12	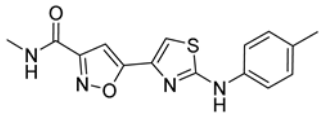	> 60 *	**19**	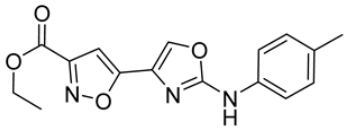	7 ± 2
13	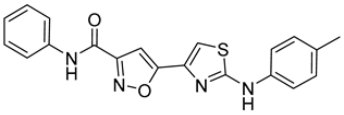	16 ± 3	**20**	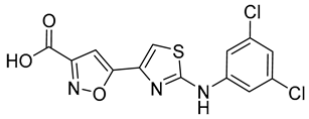	11 ± 1
14	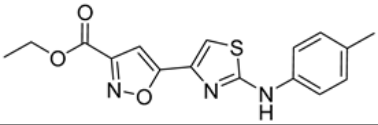	~10 *			

Chemistry

Scheme 1a. Synthetic route employed for the preparation of compounds 21a–e and 22a–e.

The target compounds 21a–e and 22a–e were synthesized following a protocol optimized in our laboratories, based on the formation of a 2-aminooxazole scaffold via condensation of suitably substituted α-bromoacetophenones with urea, followed by Buchwald–Hartwig cross-coupling with aryl halides. The synthesis commenced with a dipolar cycloaddition between 3-butyn-2-one and ethyl 2-chloro-2-(hydroxyimino)acetate in diethyl ether in the presence of triethylamine, yielding ethyl 5-acetyl-3-isoxazolecarboxylate (25). Subsequent bromination with N-bromosuccinimide (NBS) afforded intermediate 26. Microwave-assisted reaction of compound 26 with urea in dimethylformamide at 120 °C produced the key intermediate 27. This building block was then subjected to Buchwald–Hartwig coupling with variously substituted bromobenzenes to generate esters 21a–e. Final hydrolysis of the ethyl ester group using LiOH in a THF/MeOH/H_2O mixture furnished the corresponding carboxylic acids 22a–e in quantitative yields.

Structure–activity relationship considerations

This study reports the identification of effective StSAT inhibitors through a combination of virtual screening and systematic hit optimization. Following the identification of compound 5 as the most active hit from the in silico screening, an initial structure–activity relationship (SAR) analysis was conducted using a set of 13 structurally related compounds available in the in-house collection. Most of these analogues displayed enhanced affinity toward StSAT compared to the parent compound 5.

To assess the relevance of the carboxylic group, derivatives lacking this functionality were first examined. Replacement of the isoxazole-3-carboxylic motif with a pyridine ring resulted in a marked loss of activity (compound 8, IC_{50} > 400 μM), supporting the importance of this structural element. In general, the presence of a carboxylic group—either as the free acid (16, IC_{50} = 184 μM; 17, IC_{50} = 21 μM; 18, IC_{50} = 2.6 μM; 20, IC_{50} = 11 μM) or as a derived functional group such as an amide (10, IC_{50} = 9 μM; 11, IC_{50} = 26 μM; 12, IC_{50} = 60 μM; 13, IC_{50} = 16.3 μM) or ester (14, IC_{50} = 10 μM; 15, IC_{50} = 18 μM; 19, IC_{50} = 7.3 μM)—appears to be critical for

maintaining inhibitory activity, irrespective of substitution pattern. Compound 9 represents a notable exception, as it retains good potency despite lacking a carboxyl group (IC_{50} = 12 μM). These observations suggest that the electronic features associated with carboxyl-derived functionalities may favor productive interactions with the enzyme.

Among the amide derivatives, larger substituents such as phenyl or adamantyl groups at the amide nitrogen were associated with improved activity compared to smaller or unsubstituted analogues (10 and 13 versus 11 and 12). Substitution of the isoxazole ring with an N-methylpyrazole led to diminished inhibitory potency (16, IC_{50} = 184 μM; 17, IC_{50} = 21 μM) relative to the corresponding isoxazole analogues (5 and 20), indicating that the isoxazole scaffold is more favorable for enzyme binding.

Within the subset of isoxazole-3-carboxylic acid derivatives, incorporation of electron-withdrawing substituents on the phenyl ring linked to the 2-aminothiazole moiety appeared to enhance affinity (20, IC_{50} = 11 μM versus 5, IC_{50} = 110 μM), although this trend remains tentative. Esterification of the carboxyl group proved to be well tolerated (14, IC_{50} = 10 μM; 15, IC_{50} = 18 μM), regardless of substitution on the 2-aminothiazole ring. For compound 14, the IC_{50} value could only be approximated due to limited solubility. The disparity in activity between compounds 5 and 14 cannot be readily rationalized and may require the synthesis of additional analogues for clarification, as permeability differences do not appear to account for this behavior.

The most significant enhancement in activity was observed upon replacing the 2-aminothiazole moiety with a 2-aminooxazole, yielding the most potent compounds of the series (18, IC_{50} = 2.6 μM; 19, IC_{50} = 7.3 μM), corresponding to more than a 40-fold improvement compared to compound 5. These results motivated the synthesis of a focused set of additional analogues to further refine the SAR. In particular, small substituents were introduced on the phenyl ring attached to the nitrogen atom of the 2-aminooxazole, and the relative impact of ethyl ester versus free acid functionalities was evaluated.

Biochemical assessment of compounds 21a–e and 22a–e against StSAT revealed a relatively flat SAR within this subset **(Table 3).** Both ester and acid derivatives maintained comparable inhibitory activity, with ester analogues showing a slight overall advantage. Nevertheless, compound 22a—the unsubstituted acid—emerged as the most potent inhibitor in this series. Taken together, compound 22a and the related acid derivatives represent promising candidates for further development. This preference may stem from the greater metabolic stability of carboxylic acids relative to esters, which are more susceptible to hydrolysis. Additionally, these acid derivatives lack intrinsic antitubercular or antibacterial activity [39], a desirable feature to minimize off-target effects during repurposing. Introduction of small electron-withdrawing groups (21b, 21c, 22b, 22c) or electron-donating substituents (22d) on the phenyl ring had minimal influence on enzyme affinity, with the most favorable results observed for unsubstituted phenyl derivatives (21a and 22a).

Table 3. Inhibitory activity of synthesized compounds 21a–c, 21e, and 22a–e against StSAT.

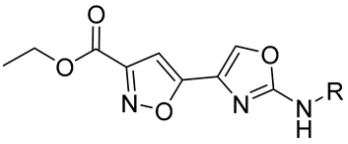

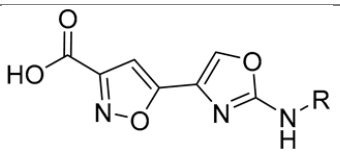

Compound	Substituent (R)	StSAT IC_{50} (μM)	Compound	R	StSAT IC_{50} (μM)
21a	Phenyl	2.68 ± 0.27	**22a**	Phenyl	1.54 ± 0.33
21b	3,5-Dichlorophenyl	2.52 ± 0.03	**22b**	3,5-Dichlorophenyl	8.03 ± 0.18
21c	4-Fluorophenyl	3.04 ± 0.37	**22c**	4-Fluorophenyl	2.51 ± 0.34
			22d	3,5-Dimethylphenyl	4.24 ±0.11
21e	Pyridin-3-yl	3.95 ± 0.65	**22e**	Pyridin-3-yl	12.02 ± 1.25

Considering that compound 5 acts as a competitive inhibitor of acetyl CoA, as predicted by computational modeling to fit into both the acetyl CoA and L-serine binding pockets, the current structure under investigation may only partially occupy the pocket. This could explain why the substitutions introduced are well tolerated, likely due to available unoccupied space within the binding cavity.

Stability of the isoxazole-oxazole core

After observing changes in the appearance of DMSO solutions over time at room temperature, we investigated the chemical stability of the compounds. To assess this, 1H NMR spectra were recorded at various time points (1 h, 2.5 h, and 20 h) for DMSO-d6 solutions (5 mg in 500 µL). Since the time needed for visible color changes in the solution varied depending on the substituent at the R2 position in series 22, three representative analogs were chosen to examine the influence of the substituent on stability: 22a (R2 = phenyl) with an unsubstituted phenyl group, 22b (R2 = 3,5-dichlorophenyl) bearing electron-withdrawing groups (EWG), and 22d (R2 = 3,5-dimethylphenyl) bearing electron-donating groups (EDG). The stability in DMSO increased in the order: 22b (< 2.5 h) < 22a (< 20 h) < 22d (< 7 days). These results indicate that EWGs, such as unsubstituted phenyl or phenyl substituted with two chlorines, lead to less stable compounds. In contrast, EDGs on the phenyl ring enhance overall molecular stability. It is proposed that the mild oxidative nature of DMSO can disrupt the oxazole ring, resulting in ring opening and subsequent complete degradation of the compound [44].

Antibacterial activity

Due to the stability concerns described above, compound 22a was not subjected to biological testing. Instead, compound 22d—which is only two-fold less potent than 22a in the biochemical assay—was evaluated for its minimum inhibitory concentration (MIC) against E. coli in both standard Mueller Hinton broth (MHB) and cysteine-deprived Middlebrook 9 (M9) medium [45]. Regrettably, no antibacterial activity was detected at concentrations up to 128 µM against two strains: E. coli ATCC25922 and S. Typhimurium ATCC14028. A likely explanation for this lack of activity is poor penetration of the compound across the Gram-negative bacterial outer membrane and cell wall—a frequent challenge in antibacterial drug development, particularly for Gram-negative pathogens.

Conclusion

By integrating virtual screening of an in-house compound collection with subsequent medicinal chemistry optimization, we identified the most potent inhibitor of StSAT reported to date. However, this lead compound exhibited limited stability upon solubilization in DMSO, prompting the selection of alternative, more stable derivatives for cellular evaluation. Among these, compound 22d emerged as the most promising candidate and was assessed for antibacterial activity against E. coli cultured in a minimal medium lacking cysteine. Despite its strong inhibitory performance in enzymatic assays, the compound failed to affect bacterial growth, an outcome likely attributable to insufficient penetration of the bacterial cell envelope.

Nevertheless, this study enabled the establishment of an initial structure–activity relationship, providing valuable insights into the molecular features governing enzyme inhibition. Ongoing synthetic efforts are focused on expanding the compound series and, in particular, on improving physicochemical properties related to membrane permeability to enhance cellular efficacy.

Acknowledgments: None

Conflict of Interest: None

Financial Support: None

Ethics Statement: None

References

1. Becker, D.; Selbach, M.; Rollenhagen, C.; Ballmaier, M.; Meyer, T.F.; Mann, M.; Bumann, D. Robust Salmonella metabolism limits possibilities for new antimicrobials. Nature 2006, 440, 303–307.
2. Bhave, D.P.; Muse, W.B.; Carroll, K.S. Drug Targets in Mycobacterial Sulfur Metabolism. Infect. Disord. Drug Targets 2007, 7, 140–158.
3. Spyrakis, F.; Singh, R.; Cozzini, P.; Campanini, B.; Salsi, E.; Felici, P.; Raboni, S.; Benedetti, P.; Cruciani, G.; Kellogg, G.; et al. Isozyme-Specific Ligands for O-acetylserine sulfhydrylase, a Novel Antibiotic Target. PLoS ONE 2013, 8, e77558.

4. Spyrakis, F.; Felici, P.; Bayden, A.S.; Salsi, E.; Miggiano, R.; Kellogg, G.E.; Cozzini, P.; Cook, P.F.; Mozzarelli, A.; Campanini, B. Fine tuning of the active site modulates specificity in the interaction of O-acetylserine sulfhydrylase isozymes with serine acetyltransferase. Biochim. Biophys. Acta 2013, 1834, 169–181.
5. Amori, L.; Katkevica, S.; Bruno, A.; Campanini, B.; Felici, P.; Mozzarelli, A.; Costantino, G. Design and synthesis of trans-2-substituted-cyclopropane-1-carboxylic acids as the first non-natural small molecule inhibitors of O-acetylserine sulfhydrylase. MedChemComm 2012, 3, 1111–1116.
6. Poyraz, O.; Jeankumar, V.U.; Saxena, S.; Schnell, R.; Haraldsson, M.; Yogeeswari, P.; Sriram, D.; Schneider, G. Structure-guided design of novel thiazolidine inhibitors of O-acetyl serine sulfhydrylase from Mycobacterium tuberculosis. J. Med. Chem. 2013, 56, 6457–6466.
7. Rabeh, W.M.; Cook, P.F. Structure and Mechanism of O-Acetylserine Sulfhydrylase. J. Biol. Chem. 2004, 279, 26803–26806.
8. Joshi, P.; Gupta, A.; Gupta, V. Insights into multifaceted activities of CysK for therapeutic interventions. 3 Biotech 2019, 9, 44.
9. Senaratne, R.H.; Silva, A.D.D.; Williams, S.J.; Mougous, J.D.; Reader, J.R.; Zhang, T.; Chan, S.; Sidders, B.; Lee, D.H.; Chan, J.; et al. 5′-Adenosinephosphosulphate reductase (CysH) protects Mycobacterium tuberculosis against free radicals during chronic infection phase in mice. Mol. Microbiol. 2006, 59, 1744–1753.
10. Lestrate, P.; Delrue, R.M.; Danese, I.; Didembourg, C.; Taminiau, B.; Mertens, P.; De Bolle, X.; Tibor, A.; Tang, C.M.; Letesson, J.J. Identification and characterization of in vivo attenuated mutants of Brucella melitensis. Mol. Microbiol. 2000, 38, 543–551.
11. Turnbull, A.L.; Surette, M.G. L-Cysteine is required for induced antibiotic resistance in actively swarming Salmonella enterica serovar Typhimurium. Microbiol. Read. Engl. 2008, 154, 3410–3419.
12. O'Connell, K.M.G.; Hodgkinson, J.T.; Sore, H.F.; Welch, M.; Salmond, G.P.C.; Spring, D.R. Combating multidrug-resistant bacteria: Current strategies for the discovery of novel antibacterials. Angew. Chem. Int. Ed Engl. 2013, 52, 10706–10733.
13. Blair, J.M.A.; Webber, M.A.; Baylay, A.J.; Ogbolu, D.O.; Piddock, L.J.V. Molecular mechanisms of antibiotic resistance. Nat. Rev. Microbiol. 2015, 13, 42–51.
14. Antibiotics: Mode of Action and Mechanisms of Resistance: Art Science. Available online: https://www.scribd.com/document/202262261/Antibiotic-Action-and-Resistance (accessed on 3 September 2019).
15. Taylor, P.L.; Wright, G.D. Novel approaches to discovery of antibacterial agents. Anim. Health Res. Rev. 2008, 9, 237–246.
16. Alekshun, M.N.; Levy, S.B. Targeting virulence to prevent infection: To kill or not to kill? Drug Discov. Today Ther. Strateg. 2004, 1, 483–489.
17. Shallcross, L.J.; Howard, S.J.; Fowler, T.; Davies, S.C. Tackling the threat of antimicrobial resistance: From policy to sustainable action. Philos. Trans. R. Soc. Lond. B. Biol. Sci. 2015, 370, 20140082.
18. Annunziato, G. Strategies to Overcome Antimicrobial Resistance (AMR) Making Use of Non-Essential Target Inhibitors: A Review. Int. J. Mol. Sci. 2019, 20, 5844.
19. Wright, G.D. Antibiotic Adjuvants: Rescuing Antibiotics from Resistance. Trends Microbiol. 2016, 24, 862–871.
20. Gill, E.E.; Franco, O.L.; Hancock, R.E.W. Antibiotic Adjuvants: Diverse Strategies for Controlling Drug-Resistant Pathogens. Chem. Biol. Drug Des. 2015, 85, 56–78.
21. Zaheer, Z.; Rahman, S.U.; Zaheer, I.; Younas, T.; Abbas, G.; Zahher, T. Antimicrobial adjuvant—An innovative strategy for handling antimicrobial resistance displayed by microbes. J. Bacteriol. Mycol. Open Access 2017, 5, 352–354.
22. Annunziato, G.; Pieroni, M.; Benoni, R.; Campanini, B.; Pertinhez, T.A.; Pecchini, C.; Bruno, A.; Magalhães, J.; Bettati, S.; Franko, N.; et al. Cyclopropane-1,2-dicarboxylic acids as new tools for the biophysical investigation of O-acetylserine sulfhydrylases by fluorimetric methods and saturation transfer difference (STD) NMR. J. Enzym. Inhib. Med. Chem. 2016, 31, 78–87.
23. Magalhães, J.; Annunziato, G.; Franko, N.; Pieroni, M.; Campanini, B.; Bruno, A.; Costantino, G. Integration of Enhanced Sampling Methods with Saturation Transfer Difference Experiments to Identify Protein Druggable Pockets. J. Chem. Inf. Model. 2018, 58, 710–723.

24. Magalhães, J.; Franko, N.; Annunziato, G.; Welch, M.; Dolan, S.K.; Bruno, A.; Mozzarelli, A.; Armao, S.; Jirgensons, A.; Pieroni, M.; et al. Discovery of novel fragments inhibiting O-acetylserine sulphhydrylase by combining scaffold hopping and ligand-based drug design. J. Enzym. Inhib. Med. Chem. 2018, 33, 1444–1452.
25. Magalhães, J.; Franko, N.; Annunziato, G.; Pieroni, M.; Benoni, R.; Nikitjuka, A.; Mozzarelli, A.; Bettati, S.; Karawajczyk, A.; Jirgensons, A.; et al. Refining the structure-activity relationships of 2-phenylcyclopropane carboxylic acids as inhibitors of O-acetylserine sulfhydrylase isoforms. J. Enzym. Inhib. Med. Chem. 2019, 34, 31–43.
26. Chen, C.; Yan, Q.; Tao, M.; Shi, H.; Han, X.; Jia, L.; Huang, Y.; Zhao, L.; Wang, C.; Ma, X.; et al. Characterization of serine acetyltransferase (CysE) from methicillin-resistant Staphylococcus aureus and inhibitory effect of two natural products on CysE. Microb. Pathog. 2019, 131, 218–226.
27. Agarwal, S.M.; Jain, R.; Bhattacharya, A.; Azam, A. Inhibitors of Escherichia coli serine acetyltransferase block proliferation of Entamoeba histolytica trophozoites. Int. J. Parasitol. 2008, 38, 137–141.
28. Palde, P.B.; Bhaskar, A.; Pedró Rosa, L.E.; Madoux, F.; Chase, P.; Gupta, V.; Spicer, T.; Scampavia, L.; Singh, A.; Carroll, K.S. First-in-Class Inhibitors of Sulfur Metabolism with Bactericidal Activity against Non-Replicating M. tuberculosis. ACS Chem. Biol. 2016, 11, 172–184.
29. Brunner, K.; Steiner, E.M.; Reshma, R.S.; Sriram, D.; Schnell, R.; Schneider, G. Profiling of in vitro activities of urea-based inhibitors against cysteine synthases from Mycobacterium tuberculosis. Bioorg. Med. Chem. Lett. 2017, 27, 4582–4587.
30. Pieroni, M.; Annunziato, G.; Beato, C.; Wouters, R.; Benoni, R.; Campanini, B.; Pertinhez, T.A.; Bettati, S.; Mozzarelli, A.; Costantino, G. Rational Design, Synthesis, and Preliminary Structure-Activity Relationships of α-Substituted-2-Phenylcyclopropane Carboxylic Acids as Inhibitors of Salmonella typhimurium O-Acetylserine Sulfhydrylase. J. Med. Chem. 2016, 59, 2567–2578.
31. Leu, L.S.; Cook, P.F. Kinetic mechanism of serine transacetylase from Salmonella typhimurium. Biochemistry 1994, 33, 2667–2671.
32. Johnson, C.M.; Huang, B.; Roderick, S.L.; Cook, P.F. Kinetic mechanism of the serine acetyltransferase from Haemophilus influenzae. Arch. Biochem. Biophys. 2004, 429, 115–122.
33. Inoue, K.; Noji, M.; Saito, K. Determination of the sites required for the allosteric inhibition of serine acetyltransferase by L-cysteine in plants. Eur. J. Biochem. 1999, 266, 220–227.
34. Tyrrell, R.; Verschueren, K.H.; Dodson, E.J.; Murshudov, G.N.; Addy, C.; Wilkinson, A.J. The structure of the cofactor-binding fragment of the LysR family member, CysB: A familiar fold with a surprising subunit arrangement. Structure 1997, 5, 1017–1032.
35. Kumar, S.; Raj, I.; Nagpal, I.; Subbarao, N.; Gourinath, S. Structural and Biochemical Studies of Serine Acetyltransferase Reveal Why the Parasite Entamoeba histolytica Cannot Form a Cysteine Synthase Complex. J. Biol. Chem. 2011, 286, 12533.
36. Pye, V.E.; Tingey, A.P.; Robson, R.L.; Moody, P.C.E. The structure and mechanism of serine acetyltransferase from Escherichia coli. J. Biol. Chem. 2004, 279, 40729–40736. Available online: https://pubmed.ncbi.nlm.nih.gov/15231846/ (accessed on 14 October 2020).
37. Magalhães, J.; Franko, N.; Raboni, S.; Annunziato, G.; Tammela, P.; Bruno, A.; Bettati, S.; Mozzarelli, A.; Pieroni, M.; Campanini, B.; et al. Inhibition of Nonessential Bacterial Targets: Discovery of a Novel Serine O-Acetyltransferase Inhibitor. ACS Med. Chem. Lett. 2020, 11, 790–797.
38. Copeland, R.A. Evaluation of Enzyme Inhibitors in Drug Discovery: A Guide for Medicinal Chemists and Pharmacologists, 2nd ed.; John Wiley & Sons: Hoboken, NJ, USA, 2013.
39. Azzali, E.; Machado, D.; Kaushik, A.; Vacondio, F.; Flisi, S.; Cabassi, C.S.; Lamichhane, G.; Viveiros, M.; Costantino, G.; Pieroni, M. Substituted N-phenyl-5-(2-(phenylamino) thiazol-4-yl) isoxazole-3-carboxamides are valuable antitubercular candidates that evade innate efflux machinery. J. Med. Chem. 2017, 60, 7108–7122.
40. Azzali, E.; Girardini, M.; Annunziato, G.; Pavone, M.; Vacondio, F.; Mori, G.; Pasca, M.R.; Costantino, G.; Pieroni, M. 2-Aminooxazole as a Novel Privileged Scaffold in Antitubercular Medicinal Chemistry. ACS Med. Chem. Lett. 2020, 11, 1435–1441.
41. Pieroni, M.; Wan, B.; Cho, S.; Franzblau, S.G.; Costantino, G. Design, synthesis and investigation on the structure–activity relationships of N-substituted 2-aminothiazole derivatives as antitubercular agents. Eur. J. Med. Chem. 2014, 72, 26–34.

42. Clinical and Laboratory Standards Institute. M07-A11: Methods for Dilution Antimicrobial Susceptibility Tests for Bacteria that Grow Aerobically, 10th ed.; Clinical and Laboratory Standards Institute: Wayne, PA, USA, 2018.
43. Denise, M.M.; Mueller, A.; Falkow, S. Persistent bacterial infections: The interface of the pathogen and the host immune system. Nat. Rev. Microbiol. 2004, 2, 747–765. Available online: https://pubmed.ncbi.nlm.nih.gov/15372085/ (accessed on 14 October 2020).
44. Turchi, I.J.; Dewar, M.J.S. Chemistry of oxazoles. Chem. Rev. 1975, 75, 389–437.
45. Balouiri, M.; Sadiki, M.; Ibnsouda, S.K. Methods for in vitro evaluating antimicrobial activity: A review. J. Pharm. Anal. 2016, 6, 71–79.